

25 MHz Ultrasonic Transducers with Lead-Free Piezoceramic, 1-3 PZT Fiber-Epoxy Composite, and PVDF Polymer Active Elements

Bahram Jadidian, Nader Marandian Hagh, Alan A. Winder, and Ahmad Safari, *Fellow, IEEE*

Abstract—This paper presents the fabrication and characterization of single-element ultrasonic transducers whose active elements are made of lead-free piezoceramic, 1-3 PZT/polymer composite and PVDF film. The lead free piezoelectric KNN-LT-LS ($\text{K}_{0.44}\text{Na}_{0.52}\text{Li}_{0.04}$)($\text{Nb}_{0.84}\text{Ta}_{0.10}\text{Sb}_{0.06}$) O_3 powders and ceramics were prepared under controlled humidity and oxygen flow rate during sintering. Due to its moderate longitudinal piezoelectric charge coefficient (175 pC/N) and k_t of 0.50, the KNN-LT-LS composition may be a good candidate for high-frequency transducer applications. PZT fibers with 25 μm diameter formed by the viscose suspension spinning process were incorporated into epoxy to fabricate 1-3 composites with the averaged $k_t = 0.64$ and $d_{33} = 400$ pC/N. Using KNN-LT-LS ceramic, 1-3 PZT fiber composite, and PVDF film, 3 different unfocused single element transducers with center frequencies of 25 MHz were fabricated. The acoustic characterization of the transducers demonstrated that wideband and low insertion loss could be obtained employing KNN-LT-LS ceramic. The -6 dB bandwidth and insertion loss were 70% and -21 dB, respectively. In comparison, the insertion loss of the ceramic transducer was much smaller than those made with 1-3 composite and PVDF film. This was attributed to closer electrical impedance match to 50 Ω and higher thickness coupling coefficient of the ceramic transducer.

I. INTRODUCTION

FOR the past 2 decades, high-frequency ultrasound imaging (HFUSI) has been the focus of many research studies to improve the image resolution to less than 10 μm . Such imaging modalities operate in the frequency range of 20 to 200 MHz. The immediate clinical applications of HFUSI are in the imaging of skin [1]–[3], gastrointestinal tract [4], [5], the arterial walls [6], [7], and anterior chamber of the eye [8], [9]. One of the main considerations for HFUSI modality is the design of a transducer with high sensitivity, signal/noise ratio (SNR), and depth of

penetration. These can be achieved by the use of a proper selection of piezoelectric material and low depth of focus using synthetic aperture focusing technique and/or B/D-scanning modes [8]. Although configured as a linear array by Ito *et al.* [10], high-frequency transducers are generally comprised of single-element piezoelectric materials in the form of ceramics, polymers, and single crystals. The main design consideration is to match the electrical impedance of the transducer to 50 ohm input/output circuitry for maximum transmit and receive sensitivity and minimum 2-way insertion loss. In the case of ceramics with high clamped capacitance, the active area of the piezoelectric ceramic must be very small (e.g., < 1 mm^2 for PZT). This is defined by the inverse relationship between the electrical impedance and the clamped capacitance of the piezomaterial. Thus, it is desirable to use a piezoceramic with low clamped permittivity and high thickness coupling coefficient. The former contributes to larger radiating area, which gives rise to a narrower beamwidth and better lateral resolution [11]. The latter contributes to improving image quality owing to a wider bandwidth and lower insertion loss.

Piezoelectric materials such as lead zirconate titanate (PZT) [9], [11]–[15], thin-film and spin-coated PVDF and P(VDF-TRFE) [16]–[18], zinc oxide [19], [20], lead titanate (PT) [21], lithium niobate (LiNbO_3) [22]–[24], and piezocomposite [25]–[30] have already been explored and shown to be appropriate choices for frequency < 200 MHz. Piezoelectric polymers offer several advantages, including low acoustic impedance and dielectric constant, flexibility, and availability in thin sheets (thickness of 9–110 μm). However, their high dielectric loss results in low sensitivity. Due to their excellent piezoelectric properties, lead zirconate titanate (PZT) ceramics have been extensively used in piezoelectric transducers. However, because of their high dielectric constant, PZT ceramics must be well matched electrically to the coaxial line and pulser/receiver systems [31]. Therefore, the application of PZT ceramic is limited to frequencies below 100 MHz [32], [33]. Foster *et al.* [33] investigated the effect of grain size of PZT ceramics on the material properties and the performance of transducers in the frequency range of 30 to 80 MHz. Using fine- and coarse-grained PZT ceramics, it was realized that, as the thickness of the ceramic resonator approached the PZT grain size, the mechanical losses increased rapidly and

Manuscript received December 24, 2007; accepted July 14, 2008. The authors acknowledge the financial support of the Glenn Howatt Foundation to the Electroceramic Laboratory of Rutgers University and the National Institute of Environmental Health Sciences (NIEHS) grant number 1R43ES012362-01 to J&W Medical.

B. Jadidian and A. A. Winder are with J&W Medical LLC, Westport, CT.

N. M. Hagh and A. Safari are with the Materials Science and Engineering Department, Rutgers, The State University of New Jersey, Piscataway, NJ (e-mail: nmhagh@rci.rutgers.edu).

Digital Object Identifier 10.1109/TUFFC.2009.1046

thickness coupling coefficient decreased. From this study, one could conclude that fine-grained piezoceramics were better choices for the fabrication of transducers resonating > 40 MHz.

The innovation of piezoelectric ceramic/polymer composites has allowed overcoming the problems associated with monolithic piezoceramics and piezopolymers in transducer applications. Combination of a piezoelectric ceramic with a polymer permits tailoring the mechanical and electrical properties of composites to satisfy the specific design requirements. In addition, a piezocomposite with a proper connectivity and ratio of each phase provides low density, high flexibility (using soft polymer), good acoustic impedance matching, moderate dielectric constant, low mechanical quality factor, and extremely high thickness coupling coefficient [34]. The mechanical and electrical properties of piezocomposites strongly depend on the characteristics of each phase and the manner in which they are connected. The connectivity (number of dimensions in which each phase is self-connected) is a key to the performance of a piezocomposite. To date, structures that have demonstrated significant piezoelectric properties for many applications, specifically medical imaging, are those with 1-3 and 2-2 connectivity.

Simple models [34], [35] for the piezoelectric charge and voltage coefficients of diphasic composites have shown that composites with 1-3 connectivity yield effective transducers. In many applications, the thickness mode resonance frequency is the most important vibration mode. In these applications, the fundamental thickness resonance frequency of the piezoelectric plate is inversely proportional to its thickness. Therefore, the thinner the plate, the higher is the thickness mode resonance frequency. To enhance the efficiency of a 1-3 piezoelectric composite, the interference of lateral resonance frequencies on the thickness resonance frequency must be minimized which, in turn, will improve the transmit and receive sensitivities of the transducer. When a piezoelectric composite vibrates at its resonance frequency, the PZT rods act as a source of waves, which propagate perpendicular to the rod axis. If the wavelengths of these transverse waves are at least 2 times higher than the periodicity of the rods, the lateral frequencies occur at higher frequencies than the thickness mode [36]. Thus, for a piezoelectric composite to vibrate uniformly and operate effectively at its resonance frequency, the piezoceramic phase must be scaled down in size. Incorporation of PZT fibers, with diameters between 10 and 15 μm , into piezoelectric composites is a promising way to attain as small a periodicity as possible in piezocomposites and to reduce the interference of lateral resonance frequencies.

High content of toxic element (Pb > 60 wt %) in lead-based piezoceramics has recently caused major environmental concerns in Europe and Japan with the challenging issues of utilization, recycling, and disposal of lead-based ferroelectrics. These environmental and safety concerns have induced a new surge in developing lead-free ferroelectrics, specifically those with properties comparable to

their lead-based counterparts. This has led to the Restriction of Hazardous Substances (RoHS) Directive, enforced in the European Union since July 2006. This directive bans new electrical and electronic equipment containing more than agreed levels of lead, cadmium, mercury, hexavalent chromium, polybrominated biphenyl (PBB), and polybrominated diphenyl ether (PBDE) flame retardants.

Recently, ceramics with perovskite structures such as $\text{Bi}_{1/2}\text{Na}_{1/2}\text{TiO}_3$ -based solid solution and alkaline niobate compounds $\text{K}_{1/2}\text{Na}_{1/2}\text{NbO}_3$ (KNN) have received considerable attention due to their higher piezoelectric properties and coupling coefficients than any other nonlead-based piezoelectric ceramics [37]–[42]. KNN is a solid solution of KNbO_3 and NaNbO_3 . The addition of potassium niobate (KN) to sodium niobate (NN) results in a ferroelectric phase with a high T_c exceeding 400°C. However it demonstrates low piezoelectric performance (d_{33} of 80 pC/N and k_p of 36%) owing to the difficulty in processing of the dense ceramics by ordinary sintering process [43], [44]. Hot pressing or hot forging of KNN has proven to be very effective in obtaining improved piezoelectric properties as compared with those obtained otherwise [42], [45]. Attempts have also been made to improve the sinterability and piezoelectric properties of KNN through A-site or B-site addition/substitutions [46]–[52]. Pioneering works on the binary and ternary systems of KNN- LiTaO_3 and KNN- LiTaO_3 - LiSbO_3 , respectively [53], [54], have explicitly shown that piezoelectric properties comparable to those of PZT can indeed be achieved. Despite its high electromechanical properties, the KNN-LT-LS system still needs a careful preparation procedure. This is attributed to the possible formation of nonstoichiometric phases of potassium niobate compositions with hygroscopic nature. A detailed investigation on the processing-property relationship in this system has shown that ceramic powder preparation and sintering process have profound effects on the physical and electromechanical properties of ceramics [55]. The electromechanical properties of this system fall in the range of $d_{33} = 130$ –315 pC/N, dielectric constant = 500–1700, $\tan\delta = 0.02$ –0.035, $k_t = 0.27$ –0.45. Eliminating the exposure of initial raw materials to humidity and sintering at high oxygen flow rate improves the properties of the ceramics. These include achieving higher piezoelectric properties and lower dielectric loss.

The aim of this paper is to present the initial results of 3 ultrasonic transducers resonating at 25 MHz. The piezoelectric materials are lead-free KNN-LS-LT, PVDF, and 1-3 PZT fiber/polymer composite. The following sections represent the organization of this paper. Section II describes the preparation and characterization of $(\text{K}_{0.44}\text{Na}_{0.52}\text{Li}_{0.04})(\text{Nb}_{0.84}\text{Ta}_{0.10}\text{Sb}_{0.06})\text{O}_3$; KNN-LT-LS ceramics. Section III explains the fabrication and electromechanical properties of 1-3 PZT fiber/epoxy composite. Section IV presents the acoustic properties of silver epoxy matching layer. Section V describes the fabrication and characterization of single-element transducers made of KNN-LS-LT, PVDF, and 1-3 composites operating at 25 MHz. Section VI presents the conclusions.

TABLE I. PROPERTIES OF KNN-LT-LS CERAMIC AND 1-3 PZT FIBER/POMPOSITE.

Material	Rel. density	d_{33} (pC/N)	$\varepsilon_{33}^T/\varepsilon_0$	$\tan\delta_{\text{free}}$	$\varepsilon_{33}^S/\varepsilon_0$	$\tan\delta_{\text{clamped}}$	k_t	K_p
KNN-LS-LT	0.96	175	644	0.022	506	0.023	0.39	0.25
1-3 PZT fiber/polymer	0.42	400	541	0.013	296	0.013	0.64	0.64

II. FABRICATION OF KNN-LT-LS CERAMICS

As stated earlier, to fabricate a single-element high-frequency transducer with large radiating area, the clamped capacitance and dielectric loss of piezoelectric ceramic must be as small as possible. Therefore, in this study, a processing condition was selected to produce ceramics with lowest dielectric constant and moderate piezoelectric properties. The detailed specifications of the sample preparation have been described in [55]. The raw materials were first heated at 220°C for 24 h. Then the 5 binary compositions of sodium niobate (NaNbO₃; NN), potassium niobate (KNbO₃; KN), potassium tantalate (KTaO₃; KT), lithium antimonate (LiSbO₃; LS), and sodium antimonate (NaSbO₃; NS) were separately prepared in dry (Ar atmosphere in glove box) atmosphere and synthesized at 800°C for 5 h. Then, the appropriate molar ratio of calcined NN, KN, KT, LS, and NS powders were mixed, ball milled in dry Acetone for 24 h, and dried overnight at 110°C. The mixed powder was then uniaxially pressed at 30 MPa and cold isostatic pressed (CIPed) at 138 MPa into 12 mm in diameter and 1.5 mm thick discs. Ceramic discs were sintered at 1150°C for 1 h in oxygen flow rate of 80 cm³/min while their top and bottom surfaces were covered with Pt foils. Using a field emission scanning electron microscope (FESEM), it was realized that the top surfaces of as-sintered bodies had sharp-cornered cubic grains. Priya *et al.* also observed similar grain morphology in potassium sodium niobate (K_{0.5}Na_{0.5}NbO₃) ceramics [56]. The grain size distribution in sintered ceramics was uniform and the average grain size was 3 μm.

After sintering, the discs were lapped on both sides to obtain 0.5 mm thick discs whose surface was coated later with Au using the gold-sputtering technique. The samples were poled at 30 kV/cm electric field for 15 min in a silicon oil bath at 100°C. The free relative permittivity ($\varepsilon_{33}^T/\varepsilon_0$) and dielectric loss were measured at room temperature and 1 kHz using an HP 4194A impedance/gain-phase analyzer (HP, Palo Alto, CA). Using a Berlincourt piezometer (Channel Products, Inc., Chesterland, OH), the piezoelectric charge coefficients were measured and averaged from at least 10 readings at different locations of either surface of each ceramic. Piezoelectric planar and thickness coupling coefficients (k_p and k_t , respectively) were calculated from the resonance and anti-resonance frequencies of the impedance traces, based on the following relations and IEEE standards [57]. The longitudinal coupling coefficient, k_{33} , was estimated from the thickness and planar coupling coefficients [1]:

$$k_{33}^2 = k_p^2 + k_t^2 - k_p^2 k_t^2 \quad (1)$$

The clamped relative permittivity ($\varepsilon_{33}^S/\varepsilon_0$) was calculated by [57]:

$$\varepsilon_{33}^S/\varepsilon_0 = (\varepsilon_{33}^T/\varepsilon_0)[(1 - k_p^2)(1 - k_t^2)] \quad (2)$$

Table I represents the physical and electromechanical properties of these samples.

III. FABRICATION AND CHARACTERIZATION OF 1-3 PZT FIBER/EPOXY COMPOSITE

Various techniques have been used to form fine fibers of 5 to 200 μm diameter [58]. However, only 3 different methods,—the sol-gel process [59]–[64], the relic process [65]–[69], and the viscous suspension spinning process (VSSP) [70]—have produced fine PZT and/or PbTiO₃ fibers. The sol-gel technique relies on the hydrolization and polycondensation of a metal alkoxide and/or metal salt precursor solution. The fibers are fabricated by extruding the high viscosity sol through a spinneret followed by drying at room temperature and firing at 700–1250°C. In forming fibers via the relic process, activated carbon fibers are saturated with a precursor solution of metal salt or alkoxide. Subsequent to drying and burning out the organic content, piezoelectric fibers are formed by sintering at 1250°C. Large quantities of continuous PZT fibers have been produced using a cost-effective method adopted from rayon technology at Advanced Cerametrics Inc. (ACI, Lambertville, NJ) [70]. With the VSSP technique, a mixture of PZT powder and cellulose xanthate (as the fugitive carrier) is extruded through the spinneret holes for the production of continuous ceramic fibers. The xanthate groups are removed from the cellulose using a solution containing sodium sulfate, zinc sulfate, and sulfuric acid dissolved in water. Once the tow is properly washed, the cellulose is very clean and will completely burn out before sintering.

In this study, PZT-5H (Morgan, Fairfield, NJ) powder with the mean particle size from 2.0 μm to 2.5 μm was used to prepare fine PZT fibers with an average diameter of 25 μm using the VSSP process. Thermogravimetry (TG) analysis of as-received fibers indicated that the organic (cellulose) was completely removed between 250 and 500°C. The green fibers were collimated, heat treated at 550°C for 4 h and at 780°C for 1 h to strengthen the sample for handling. After sintering in a lead-controlled atmosphere at 1265°C for 60 min, the sample was placed in a plastic tube and embedded with Epotek 301 epoxy (Epoxy Technology Inc., Billerica, MA). Once the epoxy was cured at room temperature for 24 h, the composite was sliced into 400 μm thick samples. Then the samples

TABLE II. THE PHYSICAL AND ACOUSTIC PROPERTIES OF SILVER EPOXY (DUPONT 4922N).

Frequency (MHz)	Velocity (m/s)	Z (MRayls)	Attenuation (dB/cm)
5.0	1663.4 ± 6.27	7.64 ± 0.029	26.88 ± 0.587
7.5	1681.8 ± 1.15	7.72 ± 0.005	36.85 ± 0.178
10.0	1686.5 ± 2.00	7.74 ± 0.009	45.17 ± 0.756
25.0	1686.5 ± 4.00	7.74 ± 0.018	113.00 ± 0.23
30.0 ²⁴ 2–3μm Pt particles/Insulcast 501	1900	7.3	138
30.0 ⁷⁷ Ablebond 16-ILV	1950	4.68	1200
30.0 ⁷⁷ Ablebond 16-ILV (Centrifuged)	1020	3.73	1000
30.0 ⁷⁷ E-Solder 3022	2110	5.46	400
30.0 ⁷⁷ E-Solder 3022 (Centrifuged)	1500	5.92	1100

were polished to 200 μm thickness and dried at 72°C for 4 h. Next, the samples were electroded using air-dried silver paint (DuPont 4922N) and poled for 10 min via the conventional method in a 60°C silicone oil bath at 40 kV/cm. Table I also represents the physical and electromechanical properties of the composites with 40 to 45 vol.% PZT fibers.

IV. PREPARATION AND CHARACTERIZATION OF ACOUSTIC MATCHING LAYER

In general, the large impedance mismatch between the ceramic resonator and the medium (tissue or water) gives rise to a large reflection coefficient of acoustic wave at the ceramic/medium interface and a narrow bandwidth transducer. Assuming $Z_{\text{Ceramic}} = 30$ MRayls and $Z_{\text{medium}} = 1.5$ MRayls, the acoustic intensity transmission coefficient is only about 18%, an acoustic coupling loss of 7.45 dB. To resolve these problems, one or more matching layers are placed between the ceramic and medium to act as an acoustic impedance down-transformer to minimize the coupling loss. When only one matching layer is used, the required acoustic impedance of the matching layer (Z_M) can be calculated using the semi-infinite [71] and infinite [72] models according to (3) and (4), respectively:

$$Z_M = \sqrt{Z_m \cdot Z_C}, \quad (3)$$

$$Z_M = \sqrt[3]{2Z_m^2 \cdot Z_C}. \quad (4)$$

For maximum transmission of acoustic waves into the medium, the thickness of the matching layer is approximately $\lambda/4$ at the desired resonance frequency [73]. Using (3) and (4), the required acoustic impedance of a matching layer for the KNN-LT-LS ceramic ($Z = 28.5$ MRayls) and water ($Z = 1.5$ MRayls) is between 5 and 6.5 MRayls.

Silver epoxy has already been used as the front matching layer [74], [75]. In this study, the DuPont 4922N (70 wt.% Pt) was cast into a plastic mold and cured at room temperature for 48 h followed by final curing at 60°C for 24 h. The sample was then removed from the mold and polished into a 25.4 mm diameter and 710 μm thick disc, and its acoustic properties were measured using the pulse/echo technique described by Selfridge [76]. Table II represents the physical and acoustic properties of silver epoxy

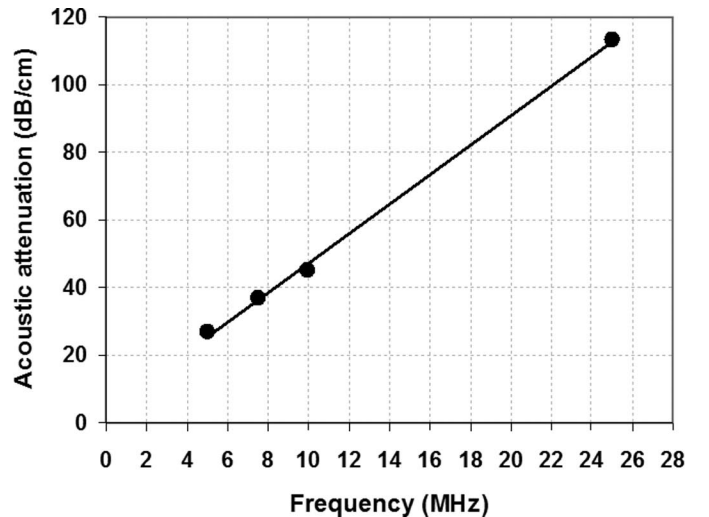


Fig. 1. Variation of acoustic attenuation of silver epoxy composite with frequency.

measured at various frequencies. Although the acoustic impedance and the longitudinal sound velocity did not change with frequency, the acoustic attenuation increased linearly with frequency, as shown in Fig. 1. Extrapolation of the data to 30 MHz results in an acoustic attenuation of 135.6 dB/cm. For comparison, the data reported in the literature for commercially available silver epoxies including the 0–3 composite prepared by Cannata [24] are shown in Table II. Although the acoustic impedance of DuPont 4922N is slightly higher than the required value (5 and 6.5 MRayls) for the KNN-LS-LT transducer, its acoustic attenuation is almost one order of magnitude lower than those reported in the literature for other commercially available silver epoxies. In addition to being a good candidate material as a matching layer, its high acoustic impedance and moderate attenuation also makes this silver epoxy a suitable material as a backing layer for piezoceramics.

V. FABRICATION AND CHARACTERIZATION OF ULTRASONIC TRANSDUCERS

A. Transducer Fabrication Process

Fig. 2(a) schematically shows the processing steps involved in the fabrication of a 25 MHz KNN-LS-LT

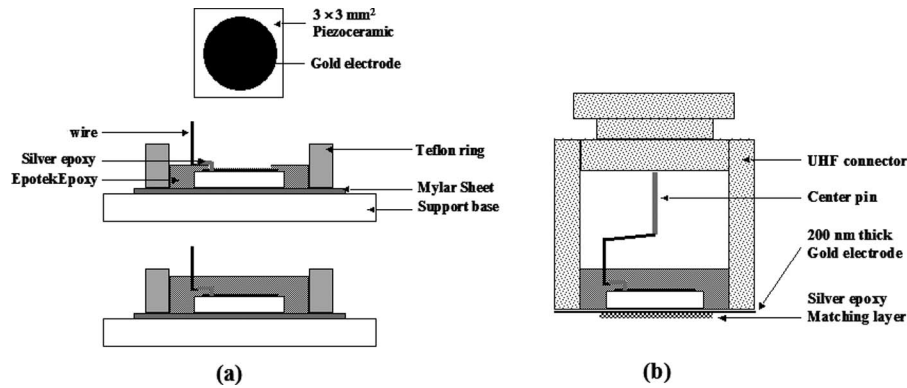


Fig. 2. Schematic representation of (a) the processing steps involved in the fabrication of the transducer and (b) the 25 MHz transducer structure.

transducer. To compensate the mass-loading effect of the matching and backing layers, a $3 \times 3 \text{ mm}^2$ ceramic prepared by the CIP procedure was lapped down to $115 \mu\text{m}$ thickness. This was slightly thinner than the $120 \mu\text{m}$ thickness required for $\lambda/2$ resonant modes. One surface of the element was covered with a template having 2.5 mm diameter hole at its center. Then a thin layer of gold electrode, $\sim 150 \text{ nm}$ thick, was sputtered onto the element. The acoustic impedance of gold, $Z = 63.8 \text{ MRayls}$ [76], is much higher than that of KNN-LT-LS ceramic. Thus, to operate at $\lambda/2$ resonance, the thickness of the gold layer had to be significantly smaller relative to that of piezoelectric material [78]. The element was secured onto a Mylar sheet with the gold electrode facing up. A Teflon ring was placed around the element and Epotek 301 was cast into the gap between the element and the ring. Before casting, the epoxy was partially cured at room temperature to permit the gold electrode to be exposed for wire attachment. After curing, a $120 \mu\text{m}$ thick copper wire was placed onto the epoxy and connected to the gold electrode using silver epoxy (DuPont 4922N). The backside of the element was refilled with Epotek 301 and cured at room temperature. The thickness of the epoxy layer on the back of the ceramic was approximately 3 mm and acted as the backing layer. The acoustic impedance and longitudinal velocity of Epotek 301 reported in [76] were 2.85 MRayls and 2640 m/s , respectively. Recently Wang [79] reported the longitudinal velocity and acoustic attenuation of Epotek 301 at 42 MHz were 2690 m/s and 17.2 dB/mm . Considering the density of cured epoxy to be 1100 Kg/m^3 , the calculated acoustic impedance would thus be equal to 2.96 MRayls . After removing the Mylar sheet and Teflon ring, the copper wire was soldered to the central pin of a UHF connector and the sample secured with Epotek epoxy. The front face of the transducer was then sputtered across with 50 nm thick gold layer to form the front electrode and connected to the body of the UHF connector. Then the element was repped at room temperature at 30 kV/cm for 10 min . To match its acoustic impedance of 6 MRayls , the silver epoxy was diluted with a small amount of n-Butylacetate (Fisher Scientific, Pittsburgh, PA) and then was painted onto the front side of the ceramic to form the matching layer. After curing, the silver epoxy was lapped

down to $\lambda/4$ thickness at 25 MHz . Fig. 2(b) schematically depicts the transducer structure.

A similar approach was taken to fabricate PVDF (Measurement Specialties Inc., Wayne, PA) and 1-3 composite transducers with diameter/thickness of the active elements $1.8 \text{ mm}/28 \mu\text{m}$ and $3 \text{ mm}/50 \mu\text{m}$, respectively. For these transducers, the Teflon ring was replaced with brass tubes fitting onto UHF connectors, their backing layers were 2 mm thick made of Epotek 301, and matching layers were not required due to their low acoustic impedance.

B. Electrical Impedance Measurement

Fig. 3(a)–(b) depict the impedance and phase angle spectra of the KNN-LS-LT transducer before and after applying a matching layer. The calculated thickness coupling coefficient of the transducer was 0.40 , which was in good agreement with that shown in Table I. This indicated that the piezoceramic regained its piezoelectric properties after repoling. The transducer was analyzed using the 1-D KLM model (PiezoCAD; Sonic Concept Inc., Woodinville, WA). The model included 2 mm thick Epotek 301 as backing material, $115 \mu\text{m}$ thick KNN-LS-LT ceramic, and $\lambda/4$ thick silver epoxy with $Z = 6 \text{ MRayls}$. Table III compares the measured and modeled impedance and phase angle of transducer with and without matching layer. A good agreement was observed between the predicted and measured values. Fig. 3(c) shows the impedance and phase angle spectra of the 1-3 PZT composite disc with 3 mm diameter. At 25 MHz , the impedance and phase angle of the composite are 11.1Ω and 61.7° . Using a clamped dielectric constant equal to 296 and a composite thickness equal to $50 \mu\text{m}$, the calculated impedance of 17.2Ω was in close agreement with the value measured. Although easily detectable for $200 \mu\text{m}$ thick composites, the detection of resonance and anti-resonance frequencies were not achievable for $50 \mu\text{m}$ thick composites. This was attributed to the effect of PZT fiber aspect ratio (diameter/height) on the composite thickness coupling coefficient and vibration modes of PZT fibers and epoxy matrix. The PZT fiber aspect ratios were 0.125 and 0.5 for $200 \mu\text{m}$ and $50 \mu\text{m}$ thick composites. According to the results of analytical analyses verified by experimental measurement that was

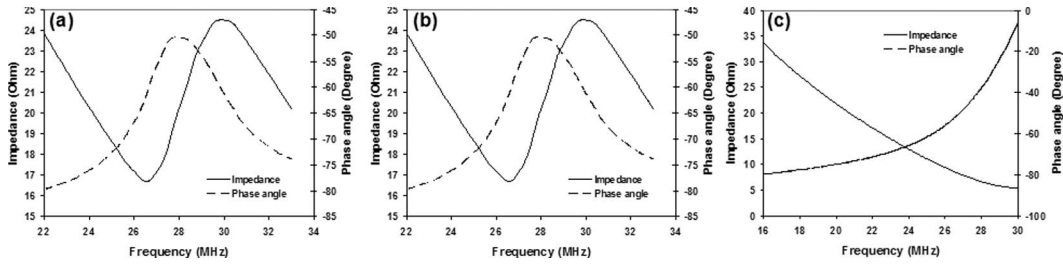


Fig. 3. The impedance and phase angle spectrums of the KNN-LT-LS transducer (a) before and (b) after putting silver epoxy matching layer onto the gold front electrode; (c) the impedance and phase angle spectrums of the 1-3 PZT composite disc.

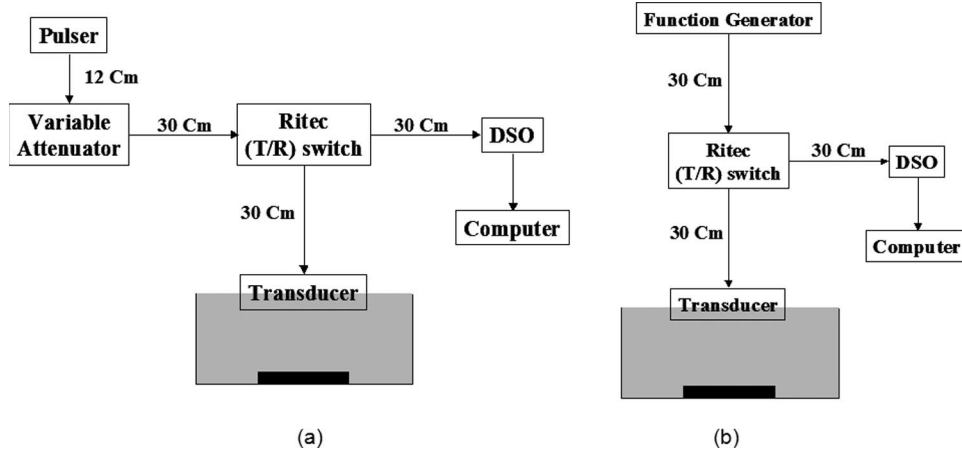


Fig. 4. (a) Pulse/echo excitation and (b) burst/echo excitation setups.

TABLE III. THE MEASURED AND MODELED IMPEDANCE AND PHASE ANGLE OF KNN-LS-LT TRANSDUCER WITH AND WITHOUT MATCHING LAYER.

Property	Ceramic with BL only		Ceramic with BL and ML	
	PiezoCAD	Measured	PiezoCAD	Measured
Z (Ω)	20.47	18.7	31.56	33.5
Phase angle ($^\circ$)	-73.7	-72.7	-77.0	-69.9

Note: BL: backing layer; ML: matching layer

carried out by Hossack and Hayward [80], the ceramic aspect ratio played an important role on the thickness coupling coefficient of 1-3 composites as well as the vibration modes of PZT pillars and their surrounding polymer. It was realized that, for composites with ceramic volume fractions less than 50%, increasing the pillar’s aspect ratio would reduce the effective k_t and longitudinal sound velocity. In addition, this was accompanied by difficulty in the detection of the thickness resonance and anti-resonance frequencies as the aspect ratio increased.

C. Ultrasonic Properties

The pulse-echo response of the transducer was measured using a conventional pulse-echo method in water at room temperature, shown in Fig. 4(a). The transducers were shock excited by a standard pulser (Model 5800PR; Panametrics, Waltham, MA) while its output voltage was

set to 60 V, employing a variable attenuator. The echo waveforms were recorded from a polished glass plate ($10 \times 10 \times 2.5 \text{ cm}^3$) by a digital oscilloscope (LeCroy 9354TM; Chestnut Ridge, NY). The frequency spectrum of the transducer echo response was obtained using the fast Fourier transform (FFT) function of the oscilloscope. The center frequency (f_c), maximum frequency (f_{max}) and the low and high frequencies (f_L and f_H , respectively) at -6 dB points were then obtained from the calculated 2-way response spectrum. For the burst excitation, the pulser was replaced with a function generator (HP8116A; Hewlett-Packard, Santa Clara, CA) and the variable attenuator removed, shown in Fig. 4(b). The transducers were excited with a 25 MHz, 1-cycle sine wave at $16 V_{p-p}$. The insertion loss was measured as described in [81] and using the setup shown in Fig. 4(b) with 25 MHz, 10-cycle sine wave burst at $16 V_{p-p}$, with $50\text{-}\Omega$ coupling of the LeCroy oscilloscope. The reflected echo waveforms were then recorded from a polished glass plate by the LeCroy oscilloscope in $1\text{-M}\Omega$ coupling.

Fig. 5 shows the time echo responses and associated frequency spectra of the KNN-LS-LT transducer, with and without matching layer. As expected, the transducer without matching layer had a very narrow -6 dB bandwidth and long -20 dB pulse length with a center frequency of $\sim 25 \text{ MHz}$, as shown in Fig. 5(a)–(b). The silver epoxy matching layer significantly improved the performance of the transducer by widening the bandwidth and shortening the pulse length, as shown in Fig. 5(c)–(d). As shown in

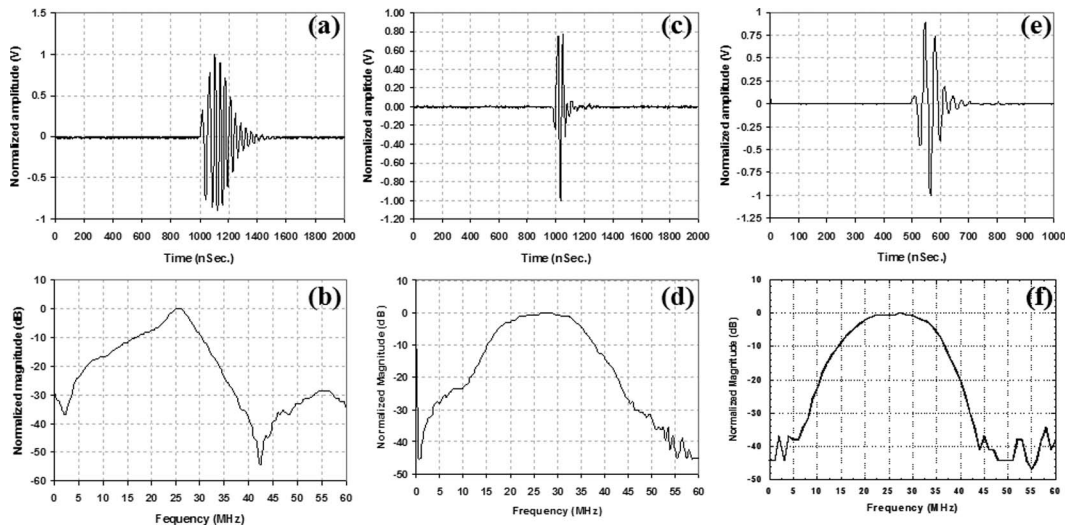


Fig. 5. The time and frequency domain spectrums of the KNN-LS-LT transducer (a)–(b) shock excitation: with backing and without matching layer; (c)–(d) shock excitation: with backing and matching layer; and (e)–(f) burst excitation: with backing and matching layer.

TABLE IV. MEASURED PARAMETERS OF 25 MHz KNN-LT-LS TRANSDUCER WITH AND WITHOUT SILVER EPOXY MATCHING LAYER (ML).

Parameter/Condition	Shock Excitation		Burst
	Without ML	With ML	Excitation With ML
f_L (MHz)	21.72	16.89	16.80
f_H (MHz)	28.10	35.77	35.00
f_0 (MHz)	25.16	26.30	25.90
–6 dB bandwidth (%)	27.38	71.80	70.30
–20 dB pulse length (ns)	376	125	124

Table IV, the center frequencies, –6 dB bandwidths, and –20 dB pulse lengths of the transducer measured with a mono-cycle pulse and one cycle sine wave burst shown in Fig. 5(e)–(f) were similar. The measured 2-way insertion loss of the transducer with matching layer after compensation for the attenuation in water (2.2×10^{-4} dB/mm.MHz²) [12] and transmission in glass plate (24% loss measured at 25 MHz) was –21.03 dB. In comparison, the bandwidth and insertion loss of KNN-LS-LT transducer were similar to those (72% and –19.5 dB, respectively) of 22 MHz transducers made of LiNbO₃ [24].

Fig. 6(a)–(b) depict the shock-excited time responses and frequency spectra of the PVDF transducer with the center frequency, compensated insertion loss, and –6 dB bandwidth of 24.5 MHz, –39.5 dB, and 108%, respectively. The acoustic impedance (~ 4 MRayls) of PVDF was a close match to that of water and thus wide –6 dB bandwidth was expected for this transducer material without matching layer.

The shock-excited time responses and frequency spectra of the 1-3 PZT fiber/polymer composite are shown in Fig. 6(c)–(d). The measured center frequency, compensated insertion loss, and –6 dB bandwidth were 24 MHz, –34 dB, and 118%, respectively. Li *et al.* [30] achieved 118% –6 dB bandwidth and –29.3 dB insertion loss for a focused 31 MHz transducer with 1-3 piezocomposite made of doped

lead titanate fibers. The transducer did not have a quarter wavelength matching layer, and its piezocomposite contained 68 vol.% fibers whose diameters were 35 μm . Meyer *et al.* [27] reported –6 dB bandwidth and insertion loss of 89% and –21 dB, respectively, for an unfocused 30 MHz 1-3 composite transducer. The composite had 45 vol.% lead lanthanum zirconate titanate (PLZT) fibers whose diameters were 17 to 30 μm in diameter. Furthermore, the deposition of $\lambda/4$ thick matching layer (parlylene C) did not have a remarkable effect on insertion loss but broadened the bandwidth. In this work, the measured acoustic impedance of the 200 μm thick 1-3 PZT fiber composites was ~ 11 MRayls. This would mean a matching layer with acoustic impedance in the range of 3.7 to 4 MRayls had to be used on the front face of the 50 μm thick composite for optimum performance (wide bandwidth and short pulse length). Achieving 118% bandwidth without employing a matching layer could thus be attributed to lower acoustic impedance of the thin composite. As explained earlier, Hossack [80] demonstrated that in 1-3 composites with low ceramic volume fraction, the sound velocity decreased with the increase of pillar’s aspect ratio. Because the density did not change with reducing the thickness, the product of density and lower sound velocity could yield composites with lower acoustic impedance. This in return would result in a better acoustic match between the composite and the medium (water).

VI. CONCLUSIONS

Lead-free KNN-LS-LT ceramics were prepared under controlled atmosphere to prevent the exposure of initial raw materials to humidity. The ceramic powder was cold isostatic pressed into discs and sintered under an oxygen flow rate of 80 cm³/min. As-sintered bodies had sharp-cornered cubic grains with uniform size distribution of 3 μm . The acoustic properties of a commercially available

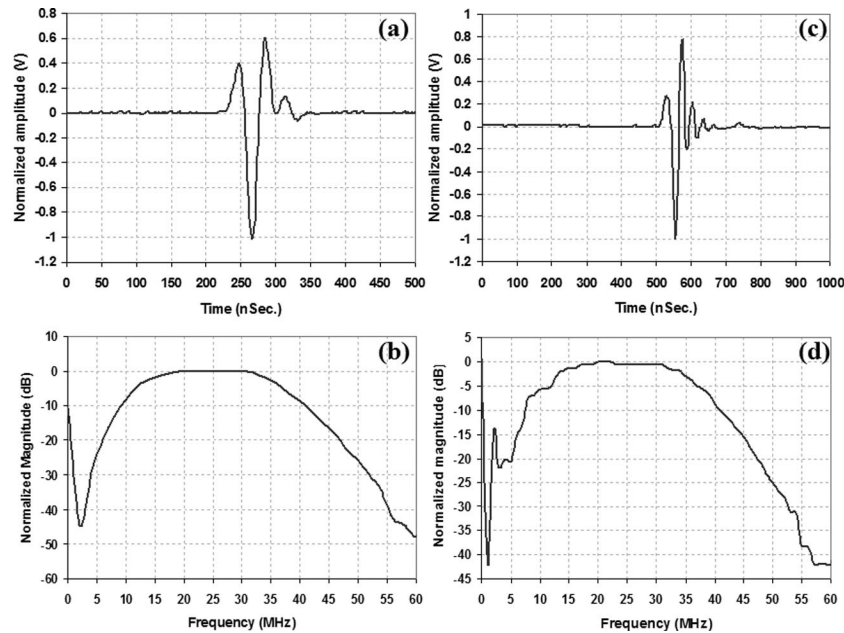


Fig. 6. The time and frequency domain spectrums of (a)–(b) the PVDF transducers and (c)–(d) the 1-3 PZT fiber/polymer composite.

silver epoxy (DuPont 422N) were characterized in frequency range of 5 to 25 MHz. Although the longitudinal sound velocity and acoustic impedance did not change, the acoustic attenuation of this silver epoxy increased linearly with frequency. In comparison, the acoustic attenuation extrapolated to 30 MHz was almost one order of magnitude lower than those reported in the literature for other commercially available silver epoxies. In addition to being a good candidate as a matching layer, its high acoustic impedance and moderate attenuation also makes this silver epoxy a suitable material as a backing layer.

Three different transducers with center-resonant frequency of 25 MHz were fabricated using cold isostatically pressed KNN-LS-LT ceramic, 1-3 PZT fiber composite, and PVDF film. Although at frequencies above 20 MHz single-element transducers are commonly made with pre-focused piezoelectric elements or focused lenses, in this study, the transducers fabricated had flat active piezoelectric materials. The acoustic characterization of the transducers demonstrated that a wideband transducer with low insertion loss could be obtained employing the nonlead KNN-LS-LT ceramic. In comparison, the insertion loss of the lead free ceramic transducer was much smaller than those made with 1-3 PZT composite and PVDF film, which was attributed to the electrical impedance of the ceramic transducer being much closer to 50 Ω and having a higher thickness coupling coefficient.

REFERENCES

- [1] C. Passmann and H. Emert, "150 MHz in vivo ultrasound of the skin: Imaging techniques and signal processing procedures," in *Proc. IEEE Ultrasonics Symp.*, 1994, pp. 1661–1664.
- [2] D. H. Turnbull, B. G. Starkoski, K. A. Harasiewicz, I. L. Semple, L. From, A. K. Gupta, D. N. Sauder, and F. S. Foster, "A 40–100 MHz B-scan ultrasound backscatter microscope for skin imaging," *Ultrasound Med. Biol.*, vol. 21, no. 1, pp. 79–88, 1995.
- [3] J. L. Semple, A. K. Gupta, L. From, K. A. Harasiewicz, D. N. Sauder, F. S. Foster, and D. H. Turnbull, "Does high-frequency (40–60 MHz) ultrasound imaging play a role in the clinical management of cutaneous melanoma?" *Ann. Plast. Surg.*, vol. 34, no. 6, pp. 599–606, June 1995.
- [4] M. J. Wiersema, C. R. Reilly, N. T. Sanghvi, R. Hawes, L. Wiersema, and C. Aust, "Twenty-five MHz gastrointestinal ultrasonography," in *Proc. IEEE Ultrasonics Symp.*, 1989, pp. 845–848.
- [5] F. E. Silverstein, R. W. Martin, M. B. Kimmey, G. C. Jiranek, D. W. Franklin, and A. Proctor, "Experimental evaluation of an endoscopic ultrasound probe: *In vitro* and *in vivo* canine studies," *Gastroenterology*, vol. 96, no. 4, pp. 1058–1062, Apr. 1989.
- [6] G. R. Lockwood, L. K. Ryan, A. I. Gotlieb, E. Lonn, I. W. Hunt, P. Lui, and F. S. Foster, "In vitro high resolution intravascular imaging in muscular and elastic arteries," *J. Am. Coll. Cardiol.*, vol. 20, pp. 153–160, 1992.
- [7] F. S. Foster, D. A. Knapik, J. C. Machado, I. M. C. Gallet, L. K. Ryan, and S. E. Nissen, "High frequency intracoronary ultrasound imaging," *Semin. Interv. Cardiol.*, vol. 2, no. 1, pp. 33–41, Mar. 1997.
- [8] C. Passmann and H. Ermert, "A 100-MHz ultrasound imaging system for dermatologic and ophthalmologic diagnostics," *IEEE Trans. Ultrason. Ferroelectr. Freq. Control*, vol. 43, no. 4, pp. 545–552, 1996.
- [9] M. Lukacs, M. Sayer, and F. S. Foster, "Single element high frequency (<50 MHz) PZT sol gel composite ultrasound transducers," *IEEE Trans. Ultrason. Ferroelectr. Freq. Control*, vol. 47, no. 1, pp. 148–159, 2000.
- [10] Y. Ito, K. Kushida, K. Suawara, and H. Takeuchi, "A 100-MHz ultrasonic transducer array using ZnO thin films," *IEEE Trans. Ultrason. Ferroelectr. Freq. Control*, vol. 42, no. 2, pp. 316–323, 1995.
- [11] M. I. Zipparo, K. K. Shung, and T. R. Shrout, "Piezoceramics for high frequency (20–100 MHz) single element imaging transducers," *IEEE Trans. Ultrason. Ferroelectr. Freq. Control*, vol. 44, no. 5, pp. 1038–1048, 1997.
- [12] G. R. Lockwood, D. H. Turnbull, and F. S. Foster, "Fabrication of high frequency spherically shaped ceramic transducers," *IEEE Trans. Ultrason. Ferroelectr. Freq. Control*, vol. 41, no. 2, pp. 231–235, 1994.
- [13] Q. Zhou, J. M. Cannata, R. J. Meyer Jr, D. J. Van Tol, S. Tagdigadapa, W. J. Hughes, K. K. Shung, and S. Trolrier-McKinstry, "Fabrication and characterization of micromachined high-frequency tonpizl transducers derived by PZT thick films," *IEEE Trans. Ultrason. Ferroelectr. Freq. Control*, vol. 52, no. 3, pp. 350–357, 2005.

- [14] Q. Q. Zhang, F. T. Djuth, Q. F. Zhou, C. H. Hu, J. H. Cha, and K. K. Shung, "High frequency broadband PZT thick film ultrasonic transducers for medical imaging applications," *Ultrasonics*, vol. 44, suppl. 1, pp. e711–e715, Dec. 2006.
- [15] T. W. Button, S. Cochran, K. J. Kirk, D. MacLennan, A. MacNeil, K. McDonald, C. Meggs, D. Rodriguez-Sanmartin, R. Webster, and D. Zhang, "Net-shape ceramic manufacturing as an aid to realize ultrasonic transducers for high-resolution medical imaging," in *Proc. IEEE Ultrasonics Symp.*, 2005, pp. 1625–1628.
- [16] L. F. Brown, R. L. Carlson, and J. M. Sempstrott, "Spin-cast P(VDF-TrFE) films for high performance medical ultrasound transducers," in *Proc. IEEE Ultrasonics Symp.*, 1997, pp. 1725–1727.
- [17] J. A. Ketterling, O. Aristizabal, D. H. Turnbull, and F. L. Lizzi, "Design and fabrication of a 40-MHz annular array transducer," *IEEE Trans. Ultrason. Ferroelectr. Freq. Control*, vol. 52, no. 4, pp. 672–681, 2005.
- [18] W. Zou, S. Holland, K. Y. Kim, and W. Sachse, "Wideband high frequency line-focus PVDF transducer for materials characterization," *Ultrasonics*, vol. 41, no. 3, pp. 157–161, May 2003.
- [19] K. Yokosawa, R. Shinomura, S. Sano, Y. Ito, S. Ishikawa, and Y. Sato, "A 120 MHz probe for tissue imaging," *Ultrason. Imaging*, vol. 18, no. 4, pp. 231–239, Oct. 1996.
- [20] Y. Ito, K. Kushida, H. Kanda, H. Takeuchi, K. Sugawara, and H. Onozato, "Thin-film ZnO ultrasonic transducer arrays for operation at 100 MHz," *Ferroelectrics*, vol. 134, pp. 325–330, 1992.
- [21] R. Meyer, R. Newnham, S. Alkoy, and T. Ritter, and J. Cochran Jr., "Pre-focused lead titanate >25 MHz single-element transducers from hollow spheres," *IEEE Trans. Ultrason. Ferroelectr. Freq. Control*, vol. 48, no. 2, pp. 488–493, 2001.
- [22] D. A. Knapik, B. Starkoski, C. J. Pavlin, and F. S. Foster, "A real-time 200 MHz ultrasound B-scan imager," in *Proc. IEEE Ultrasonics Symp.*, 1997, pp. 1457–1460.
- [23] D. A. Knapik, B. Starkoski, C. J. Pavlin, and F. S. Foster, "A 100–200 MHz ultrasound biomicroscope," *IEEE Trans. Ultrason. Ferroelectr. Freq. Control*, vol. 47, no. 6, pp. 1540–1549, 2000.
- [24] J. M. Cannata, T. A. Ritter, W.-H. Chen, R. H. Silverman, and K. K. Shung, "Design of efficient, broadband single-element (20–80 MHz) ultrasonic transducers for medical imaging," *IEEE Trans. Ultrason. Ferroelectr. Freq. Control*, vol. 50, no. 11, pp. 1548–1557, 2003.
- [25] R. Liu, K. A. Harasiewicz, and F. S. Foster, "Interdigital pair bonding for high frequency (20–50 MHz) ultrasonic composite transducers," *IEEE Trans. Ultrason. Ferroelectr. Freq. Control*, vol. 48, no. 1, pp. 299–306, 2001.
- [26] T. A. Ritter, K. K. Shung, R. T. Tutwiler, and T. R. Shrout, "Medical imaging arrays for frequencies above 25 MHz," in *Proc. IEEE Ultrasonics Symp.*, 1999, pp. 1203–1207.
- [27] R. Meyer, Jr., S. Alkoy, and R. Newnham, "Development of materials and composites for >25 MHz single element transducers," in *Proc. IEEE Ultrasonics Symp.*, 1999, pp. 1299–1302.
- [28] A. Nguyen-Dinh, L. Ratsimandresy, P. Mauchamp, R. Dufait, A. Flesch, and M. Lethiecq, "High frequency piezo-composite transducer array designed for ultrasound scanning applications," in *Proc. IEEE Ultrasonics Symp.*, 1996, pp. 943–947.
- [29] J.-Z. Zhao, C. H. F. Alves, K. A. Snook, J. M. Cannata, and W.-H. Chen, R. J. Meyer, Jr., S. Ayyappan, T. A. Ritter, and K. K. Shung, "Performance of 50 MHz transducers incorporating fiber composite, PVDF, PbTiO₃ and LiNbO₃," in *Proc. IEEE Ultrasonics Symp.*, 1999, vol. 2, pp. 1185–1190.
- [30] K. Li, H. L. W. Chan, and C. L. Choy, "Samarium and manganese-doped lead titanate ceramic fiber/epoxy 1-3 composite for high-frequency transducer application," *IEEE Trans. Ultrason. Ferroelectr. Freq. Control*, vol. 50, no. 10, pp. 1371–1376, 2003.
- [31] M. Lethiecq, G. Feuillard, L. Ratsimandresy, A. Nguyen-Dinh, L. Pardo, J. Ricote, B. Andersen, and C. Millar, "Miniature high frequency array transducers based on new fine grain ceramics," in *Proc. IEEE Ultrasonics Symp.*, 1994, pp. 1009–1013.
- [32] F. S. Foster, C. J. Pavlin, G. R. Lockwood, L. K. Ryan, K. A. Harasiewicz, L. R. Berube, and A. M. Rauth, "Principles and applications of ultrasound backscatter microscopy," *IEEE Trans. Ultrason. Ferroelectr. Freq. Control*, vol. 40, no. 5, pp. 608–617, 1993.
- [33] F. S. Foster, L. K. Ryan, and D. H. Turnbull, "Characterization of lead zirconate titanate ceramics for use in miniature high frequency (20–80 MHz) transducers," *IEEE Trans. Ultrason. Ferroelectr. Freq. Control*, vol. 38, no. 5, pp. 446–453, 1991.
- [34] W. A. Smith, "The role of piezocomposites in ultrasonic transducers," in *Proc. IEEE Ultrasonics Symp.*, 1989, vol. 2, pp. 755–766.
- [35] W. A. Smith and B. A. Auld, "Modeling 1-3 composite piezoelectrics: Thickness-mode oscillations," *IEEE Trans. Ultrason. Ferroelectr. Freq. Control*, vol. 38, no. 1, pp. 40–47, 1991.
- [36] T. R. Gururaja, W. A. Schulze, L. E. Cross, R. E. Newnham, B. A. Auld, and Y. J. Wang, "Piezoelectric composite materials for ultrasonic transducer applications. Part I: Resonant modes of vibration of PZT rod-polymer composites," *IEEE Trans. Ultrason. Ferroelectr. Freq. Control*, vol. SU-32, no. 4, pp. 481–498, 1985.
- [37] C. Duran, S. Trolier-McKinstry, and G. L. Messing, "Fabrication and electrical properties of textured Sr_{0.53}Ba_{0.47}Nb₂O₆ ceramics by templated grain growth," *J. Am. Ceram. Soc.*, vol. 83, no. 9, pp. 2203–2213, 2000.
- [38] G. A. Smolenski, V. A. Isupov, A. I. Agranovskaya, and N. N. Krainik, "New ferroelectrics of complex composition IV," *Sov. Phys. Solid State*, vol. 2, no. 11, pp. 2651–2654, 1961.
- [39] H. Nagata, M. Yoshida, Y. Makiuchi, and T. Takenaka, "Large piezoelectric constant and high curie temperature of lead-free piezoelectric ceramic ternary system based on bismuth sodium titanate-bismuth potassium titanate-barium titanate near the morphotropic phase boundary," *Jpn. J. Appl. Phys.*, vol. 42, no. 12, pp. 7401–7403, 2003.
- [40] G. Shirane, R. Newnham, and R. Pepinsky, "Dielectric properties and phase transitions of NaNbO₃ and (Na,K)NbO₃," *Phys. Rev.*, vol. 96, no. 3, pp. 581–588, 1954.
- [41] L. Egerton and D. M. Dillon, "Piezoelectric and dielectric properties of the ceramics in the system potassium-sodium niobate," *J. Am. Ceram. Soc.*, vol. 42, no. 9, pp. 438–442, 1959.
- [42] R. E. Jaeger and L. Egerton, "Hot pressing of potassium-sodium niobates," *J. Am. Ceram. Soc.*, vol. 45, no. 5, pp. 209–213, May 1962.
- [43] M. Kosec and D. Kolar, "On activated sintering and electrical properties of KNbO₃," *Mater. Res. Bull.*, vol. 10, no. 5, pp. 335–340, 1975.
- [44] H. Birol, D. Damjanovic, and N. Setter, "Preparation and characterization of (K_{0.5}Na_{0.5})NbO₃ ceramics," *J. Eur. Ceram. Soc.*, vol. 26, no. 6, pp. 861–866, 2006.
- [45] S. Z. Ahn and W. A. Schulze, "Conventionally sintered (K_{0.5}Na_{0.5})NbO₃ with barium additions," *Commun. Am. Ceram. Soc.*, vol. 70, no. 1, pp. C18–C21, 1987.
- [46] V. Bobnar, B. Malic, J. Holc, and M. Kosec, "Electrostrictive effect in lead-free relaxor K_{0.5}Na_{0.5}NaBO₃-SrTiO₃ ceramic system," *J. Appl. Phys.*, vol. 98, no. 1, art. no. 024113, 2005.
- [47] M. Matsubara, T. Yamaguchi, K. Kikuta, and S. Hirano, "Sinterability and piezoelectric properties of (K,Na)NbO₃ ceramics with novel sintering aid," *Jpn. J. Appl. Phys.*, vol. 43, no. 10, pp. 7159–7163, 2004.
- [48] M. Matsubara, T. Yamaguchi, K. Kikuta, and S. Hirano, "Sintering and piezoelectric properties of potassium-sodium niobate ceramics with newly developed sintering aid," *Jpn. J. Appl. Phys.*, vol. 44, no. 1A, pp. 258–263, 2005.
- [49] M. Matsubara, K. Kikuta, and S. Hirano, "Piezoelectric properties of (K_{0.5}Na_{0.5})(Nb_{1-x}Ta_x)O₃-K_{5/4}Cu_{1/3}Ta₁₀O₂₉ ceramics," *J. Appl. Phys.*, vol. 97, no. 11, art. no. 114105, 2005.
- [50] M. Matsubara, T. Yamaguchi, K. Kikuta, and S. Hirano, "Effect of Li⁺ substitution on the piezoelectric properties of potassium sodium niobate ceramics," *Jpn. J. Appl. Phys.*, vol. 44, no. 8, pp. 6136–6142, 2005.
- [51] S.-H. Park, C.-W. Ahn, S. Nahm, and J.-S. Song, "Microstructure and piezoelectric properties of ZnO-Added (Na_{0.5}K_{0.5})NbO₃ ceramics," *Jpn. J. Appl. Phys.*, vol. 43, no. 8B, pp. L1072–L1074, 2004.
- [52] K.-I. Kakimoto, I. Masuda, and H. Ohsato, "Lead-free KNbO₃ piezoceramics synthesized by pressure-less sintering," *J. Eur. Ceram. Soc.*, vol. 25, no. 12, pp. 2719–2722, 2005.
- [53] Y. Guo, K.-I. Kakimoto, and H. Ohsato, "(K_{0.5}Na_{0.5})NbO₃-LiTaO₃ lead-free piezoelectric ceramics," *Mater. Lett.*, vol. 59, pp. 241–244, 2005.
- [54] Y. Saito, H. Takao, T. Tani, T. Nanoyama, K. Takatori, T. Homma, T. Nagaya, and M. Nakamura, "Lead-free piezoceramics," *Nature*, vol. 432, pp. 84–87, 2004.
- [55] N. Marandian Hagh, B. Jadidian, and A. Safari, "Property-processing relationship in lead-free (K, Na, Li)NO₃-solid solution system," *J. Electroceram.*, vol. 18, no. 3–4, pp. 339–346, 2007.
- [56] S. Priya, A. Ando, and K. Uchino, "Development in dielectric materials and electronic devices," in *Ceramic Trans.*, vol. 167, K. M. Nair, R. Guo, A. S. Bhalla, S. I. Hirano, and D. Suvorov, Eds. Indianapolis, IN: The American Ceramic Society, 2005, p. 223–233.

- [57] *IEEE and American National Standards Institute Standards on Piezoelectricity*, ANSI/IEEE Standard 176, 1987.
- [58] C. LaCourse, "Continuous filament fibers by the sol-gel process," in *Sol-gel Technology for Thin Films, Fibers, Preforms, Electronics and Speciality Shapes*, Lisa C. Klein, Ed. Park Ridge, NJ: Noyes Publications, 1988.
- [59] S. Yoshikawa, U. Selvaraj, P. Moses, Q. Jiang, and T. Shrout, "Pb(Zr, Ti)O₃ [PZT] fibers-fabrication and properties," *Ferroelectrics*, vol. 154, no. 1, pp. 325–330, 1994.
- [60] S. Yoshikawa, U. Selvaraj, P. Moses, and T. Shrout, "Pb(Zr, Ti)O₃ [PZT] fibers-formation and property measurement methods," in *Proc. 6th U.S.–Japan Sem. Dielectric and Piezoelectric Ceramics*, 1993, internal publication, pp. 332–335.
- [61] U. Yoshikawa, Selvaraj, K. G. Brooks, and S. K. Kurtz, "Piezoelectric PZT tubes and fibers for passive vibrational damping," in *Proc. IEEE Ultrasonics Symp.*, 1992, pp. 269–272.
- [62] U. Selvaraj, A. V. Parasadarao, S. Komarneni, K. Brooks, and S. Kurtz, "Sol-gel processing of PbTiO₃ and Pb(Zr_{0.52}Ti_{0.48})O₃ fibers," *J. Mater. Res.*, vol. 7, no. 4, pp. 992–996, 1992.
- [63] L. Del Olmo and M. L. Calzada, "PbTiO₃ ceramic fibers prepared from a sol-gel process as piezoelectric materials," *J. Non-Cryst. Solids*, vol. 121, pp. 424–427, 1990.
- [64] S. Chevasatn and S. J. Milne, "Synthesis and characterization of PbTiO₃ and Ca and Mn modified PbTiO₃ fibers produced by extrusion of diol based gels," *J. Math. Sci.*, vol. 29, no. 14, pp. 3621–3629, 1994.
- [65] S. S. Livneh, S. M. Ting, and A. Safari, "Development of fine scale and large area piezoelectric ceramic fiber/polymer composites for transducer applications," *Ferroelectrics*, vol. 157, no. 1, pp. 421–426, 1994.
- [66] R. J. Card, "Preparation of hollow ceramic fibers," *Adv. Cer. Mat.*, vol. 3, no. 1, pp. 29–31, 1988.
- [67] R. J. Card and M. P. O'Tool, "Solid ceramic fibers via impregnation of activated carbon fibers," *J. Am. Ceram. Soc.*, vol. 73, no. 3, pp. 665–668, 1990.
- [68] S. Livneh, V. F. Janas, and A. Safari, "Development of fine scale PZT ceramic fiber/polymer shell composite transducers," *J. Am. Ceram. Soc.*, vol. 78, no. 7, pp. 1900–1906, 1995.
- [69] S. M. Ting, "Development of large area fine scale piezoelectric ceramic fiber/polymer composites for transducer applications," M. S. thesis, Ceram. Eng., Rutgers Univ., Piscataway, NJ, 1995.
- [70] R. Cass, "Fabrication of continuous ceramic fiber by the viscous suspension spinning Process," *Am. Ceram. Soc. Bul.*, vol. 70, no. 3, pp. 424–429, 1991.
- [71] J. H. Goll, "The design of broad-band fluid-loaded ultrasonic transducers," *IEEE Trans. Sonics Ultrason.*, vol. SU-26, no. 6, pp. 385–393, 1979.
- [72] J. Souquet, P. Defranould, and J. Desbois, "Design of low-loss wide-band ultrasonic transducers for noninvasive medical application," *IEEE Trans. Sonics Ultrason.*, vol. SU-26, no. 2, pp. 75–81, 1979.
- [73] M. G. Grewe, "Acoustic matching and backing layers for medical ultrasonic transducers," M.S. thesis, Pennsylvania State Univ., State College, PA, 1989.
- [74] J. M. Cannata, T. A. Ritter, W.-H. Chen, and K. K. Shung, "Design of focused single element (50–100 MHz) transducers using lithium niobate," in *Proc. IEEE Ultrasonics Symp.*, 2000, pp. 1129–1133.
- [75] K. A. Snook, J.-Z. Zhao, C. H. F. Alves, J. M. Cannata, W.-H. Chen, R. J. Meyer Jr., T. A. Ritter, and K. K. Shung, "Design, fabrication, and evaluation of high frequency, single-element transducers incorporating different materials," *IEEE Trans. Ultrason. Ferroelectr. Freq. Control*, vol. 49, no. 2, pp. 169–175, 2002.
- [76] A. R. Selfridge, "Approximate material properties in isotropic materials," *IEEE Trans. Sonics Ultrason.*, vol. 32, no. 3, pp. 381–394, 1985.
- [77] H. Wang, T. Ritter, W. Cao, and K. K. Shung, "High frequency properties of passive materials for ultrasonic transducers," *IEEE Trans. Ultrason. Ferroelectr. Freq. Control*, vol. 48, no. 1, pp. 78–84, 2001.
- [78] L. F. Brown, "Design consideration for piezoelectric polymer ultrasound transducers," *IEEE Trans. Ultrason. Ferroelectr. Freq. Control*, vol. 47, no. 6, pp. 1377–1396, 2000.
- [79] H. Wang and W. Cao, "Characterizing ultra-thin matching layers of high-frequency ultrasonic transducer based on impedance matching principle," *IEEE Trans. Ultrason. Ferroelectr. Freq. Control*, vol. 51, no. 2, pp. 211–215, 2004.

- [80] J. A. Hossack and G. Hayward, "Finite-element analysis of 1-3 composite transducers," *IEEE Trans. Ultrason. Ferroelectr. Freq. Control*, vol. 38, no. 6, pp. 618–629, 1991.
- [81] M. D. Sherar and F. S. Foster, "The design and fabrication of high frequency poly(vinylidene fluoride) transducers," *Ultrason. Imag.*, vol. 11, no. 2, pp. 75–94, 1989.



Bahram Jadidian was born in Tehran, Iran. He received the B.S. degree in ceramic and materials science from the University of Science and Technology, Tehran, Iran, in 1991. He received the M.S. and Ph.D. degrees in ceramic and materials science in 1997 and 1998, both from Rutgers, the State University of New Jersey. He worked in the Department of Ceramic and Materials Science as a research associate between 1998 and 1999. He was cofounder, president, and chief technical scientist of Layered Manufacturing Inc. from 1999 to 2002. He has been the president and chief technical scientist of J&W Medical, Westport, CT, since 2002. His current interests are biomedical imaging, ultrasonic transducers for therapeutic applications, piezoelectric actuators and sensors, and piezoelectric micromachined ultrasonic transducers.



Nader Marandian Hagh received his M.S. and Ph.D. degrees in materials science and engineering in 2004 and 2006, both from Rutgers, The State University of New Jersey. During his graduate study at Rutgers, he worked on numerous projects such as single crystal growth of piezoelectric ceramics, development of the anisometric templates for different piezoelectric systems to improve the electromechanical properties through microstructure texturing, and extensive research on lead-free piezoelectric ceramics and transducers based on bismuth sodium titanate and alkali niobate compounds. Currently, Nader is working at the Energy Storage Research Group (ESRG) of the Materials Science and Engineering Department at Rutgers University. His research interests are piezoelectric ceramics and ultrasonic transducers for medical applications, piezoelectric actuators and sensors, and nano-structured materials for high-energy storage devices.



Alan A. Winder holds a master's degree in electrical engineering (MEE) from the Polytechnic Institute of New York (1969) and a bachelor's degree in electrical engineering (BEE) from the City College of New York (1959). In addition, Mr. Winder completed the Medical Ultrasound Education Program at Thomas Jefferson University Hospital in Philadelphia, PA, in 1996.

Mr. Winder has been the vice president and managing director of J&W Medical LLC since 2002 and is an expert in the fields of diagnostic/therapeutic ultrasound and sonar. Prior to his association with J&W Medical, he was president and chief scientist of Acoustic Sciences Associates (ASA) in Westport, CT, from 1992 to 2002. Prior to his work with ASA, Mr. Winder was the founder and president (1972–1993) of MSB Systems, Inc. (Norwalk, CT). MSB conducted advanced research and development in sonar and medical diagnostic ultrasound for the Department of Defense (DARPA, ONR, NAVSEA, NUWC, NRL, NADC, and NMRDC). Prior to MSB, Mr. Winder was director of research (1969–1972) of EDO Corporation (College Point, NY), where he formulated and managed all IRAD undersea warfare programs and successfully marketed company sonar systems to NATO countries, South America, and Japan. Mr. Winder has been issued seven U.S. patents, with an additional four pending, in diagnostic and therapeutic ultrasound. He has been serving on the board of directors of the Ultrasonics Industry Association (UIA) since 2000 and as co-chairman of the medical session at the UIA's annual meeting since 2003.



Ahmad Safari (F'05) holds a Ph.D. degree in solid state science from The Pennsylvania State University (1983). He is a distinguished professor (PII) of materials science and engineering, and director of the Glenn Howatt Electroceramic Laboratory at Rutgers University. He is also chair of the UFFC Society's conferences committee and an associate editor of the *IEEE Transactions on Ultrasonics, Ferroelectrics, and Frequency Control*. His main fields of interest include electroceramic materials for dielectric, piezoelectric, and ferro-

electric applications; ferroelectric thin and thick films; ceramic-polymer composites for transducers, sensors, and actuators; and rapid prototyping and direct writing of advanced functional ceramics. Dr. Safari has published more than 300 refereed journal articles and has been granted 18 U.S. patents. He is a Fellow of IEEE-UFFC, American Ceramic Society; Centennial Fellow of the College of Earth and Mineral Science, The Pennsylvania State University; and past president of the IEEE Ultrasonics, Ferroelectrics, and Frequency Control Society. He chaired the 7th U.S.-Japan Meeting on Ferroelectric and Dielectric Materials (1995) and the 10th IEEE International Symposium on the Applications of Ferroelectrics (1996).